Journal of Radiation Research, Vol. 58, No. 4, 2017, pp. 412–420
doi: 10.1093/jrr/rrw084
Advance Access Publication: 3 February 2017

Acquisition of radioresistance by IL-6 treatment is caused by suppression of oxidative stress derived from mitochondria after γ-irradiation

Yuki Tamari[1], Genro Kashino[2*] and Hiromu Mori[1]

[1]Department of Radiology, Faculty of Medicine, Oita University, 1-1 Idaigaoka, Hasama-machi, Yufu, Oita 879-5593, Japan
[2]Advanced Molecular Imaging Center, Faculty of Medicine, Oita University, 1-1 Idaigaoka, Hasama-machi, Yufu, Oita 879-5593, Japan
*Corresponding author. Advanced Molecular Imaging Center, Faculty of Medicine, Oita University, 1-1 Idaigaoka, Hasama-machi, Yufu, Oita 879-5593, Japan. Tel: +81-97-586-6318; Fax: +81-97-586-6314; Email: kashino@oita-u.ac.jp
Received April 14, 2016; Revised June 6, 2016; Editorial Decision July 7, 2016

ABSTRACT

Interleukin (IL)-6 is a multifunctional cytokine and is one of the radiation-induced bystander factors. This study aimed to clarify the mechanism of acquisition of radioresistance through the control of reactive oxygen species (ROS) by IL-6. We used a rat glioma cell line (C6) as tumor cells and a rat astrocyte cell line (RNB) as non-tumor cells. Our results showed that the surviving fraction of C6 cells after 6 Gy irradiation was increased by the addition of IL-6, but that this was not the case in RNB cells. In addition, the number of 53BP1 foci in C6 cells at 30 min after γ-irradiation were decreased by IL-6. Levels of ROS in whole C6 cells, and superoxide in the mitochondria of C6 cells immediately after γ-irradiation, were reduced by IL-6, but this was not observed in RNB cells. The mitochondrial membrane potential detected by JC-1 in C6 and RNB cells was inhibited by IL-6 alone. Therefore, it was concluded that IL-6 leads specifically to radioresistance in tumor cells by inhibition of increases in ROS after γ-irradiation.

KEYWORDS: IL-6, radioresistance, ROS, mitochondria

INTRODUCTION

Interleukin (IL)-6 is one of the cytokines controlling humoral immunity and has multiple functions, such as immune and inflammatory responses [1], anti-apoptosis [2], and malignant progression [3] of cancer cells. In addition, it has been reported that IL-6 levels are increased in various tumors such as glioblastoma [4], liver cancer [5], prostate cancer [6] and lung cancer [7]. Recently, it was reported that IL-6 is associated with the acquisition of radioresistance by tumors [8]. IL-6 transmits a signal by interacting with a specific binding receptor IL-6-R and signal transducer gp130 extracellularly. IL-6 is a major activator of the JAK signal transducer and activator of transcription 3 (STAT3) signaling pathway. Various mechanisms have been clarified for IL-6, but the mechanism through which IL-6 enhances the radioresistance of tumors has not yet been clarified.

The radiation-induced bystander effect is a phenomenon in which non-irradiated cells exhibit various biological stress profiles similar to nearby irradiated cells because of the receipt of bystander factors from the irradiated cells. It has been reported that the bystander effect can be mediated via gap junction–mediated cell–cell communications [9] and also via soluble transmissible factors secreted from irradiated cells [10, 11]. It was suggested that the influences of the bystander effect include apoptosis [12], mutation [13], chromosome aberration [14], DNA double-strand breaks [15], and micronuclei formation [16]. In recent years, it was reported that the acquisition of radioresistance was one of the influences of the bystander effect [17]. Various molecules, such as transforming growth factor-beta (TGF-β) [18], tumor necrosis factor-alpha (TNF-α) [19], IL-6 [20], IL-33 [21] and reactive oxygen species (ROS) [22] are included among the bystander factors.

Mitochondria synthesize ATP and play important roles in *in vivo* energy production. Furthermore, mitochondria have a significant impact on the expression of biologically active factors, with a large amount of ROS included in this activity. ROS are produced during normal metabolism, especially as a consequence of aerobic respiration in mitochondria. ROS are necessary in aerobic organisms for cell signaling pathways and for killing invading pathogens, but it is thought that high concentrations of ROS result in oxidative stress.

This oxidative stress leads to damage to macromolecules such as DNA, proteins and lipids [23–25]. In addition, it was reported that the generation of mitochondrial ROS in a cell increases after irradiation [26]. Therefore, it is plausible that the generation of mitochondrial ROS affects events such as the indirect action of ionizing radiation or DNA damage responses after irradiation. However, the mechanism of DNA damage response through mitochondrial ROS is not fully understood.

Glioma is an adaptation disease of radiation therapy. Recovery becomes difficult due to acquisition of radioresistance during radiation therapy for glioma [27, 28]. In the present study, we showed the acquisition of radioresistance by treatment with IL-6 in C6 glioma cells, but not in non-tumor rat astrocyte cell line (RNB) cells. This phenomenon is thought to be brought about by the suppression of mitochondrial function.

MATERIALS AND METHODS

Cell culture and reagents

Rat glioma cells (C6) were obtained from Dr Takeshi Kondoh, Kobe University. Rat astrocyte cells (RNB) were obtained from JCRB Cell Bank (Osaka, Japan). These cells were cultured in Dulbecco's modified Eagle's medium (DMEM; Wako, Osaka, Japan) supplemented with 10% fetal bovine serum (FBS; HyClone Laboratories, Inc., Logan, USA). Cultures were maintained at 37°C in a humidified 5% CO_2 incubator. Recombinant IL-6 was purchased from Wako (Osaka, Japan) and was added at a concentration of 40 ng/ml after 6 h of serum starvation.

Irradiation

After 24 h treatment with recombinant IL-6, C6 and RNB cells were irradiated with ^{137}Cs γ-rays (Gammacell 40, Marubeni, Tokyo, Japan).

Bio-Plex assay

A Bio-Plex Pro rat cytokine 24-plex panel (Biorad, Japan, Tokyo, Japan) was used to perform exhaustive analysis of cytokine levels. The cells were irradiated with 4 Gy, and the culture medium was collected 24, 48, 72 and 96 h later. Twenty-four kinds of cytokine (IL-1α, IL-1β, IL-2, IL-4, IL-5, IL-6, IL-7, IL-10, IL-12, IL-13, IL-17, IL-18, EPO, G-CSF, GM-CSF, GRO/KC, IFN-γ, M-CSF, MIP-1α, MIP-3α, RANTES, TNF-α, VEGF and MCP-1) were checked in this analysis, which was performed in accordance with the manufacturer's instructions.

Colony-formation assay

To investigate the radiosensitivity of the cells, we performed colony-formation assays. Briefly, 5×10^5 cells were seeded onto a T-25 flask (25 cm^2, FALCON Becton Dickinson, Franklin Lakes, NJ) and were maintained at 37°C in a humidified atmosphere with 5% CO_2 overnight. The next day, the medium was changed for fresh medium without FBS, and recombinant IL-6 was added 6 h later. After incubation for 24 h, the cells were irradiated with 6 Gy of γ-rays. The cells were trypsinized, and detached cells were collected and cultured in 6-well plates (Becton Dickinson), with an appropriate cell count depending on the survival rate (non-irradiated: 100, 6 Gy: 1000) for 10–12 days. After culturing, the plates were fixed with methanol and stained with 5% Giemsa solution. Colonies consisting of at least 50 cells were counted. The survival fraction was calculated from the plating efficiency.

53BP1 focus assay

To estimate the induction of DNA double-strand breaks immediately after irradiation, cells on 22 × 22 mm cover slips in 35 mm dishes were irradiated with 1 Gy of γ-rays. At 0.5, 2 or 24 h after irradiation, the cells were fixed with 4% formaldehyde (Wako) in phosphate-buffered saline (PBS). Then, the cells were permeabilized for 10 min in 0.5% Triton X-100 in PBS and washed with PBS. The cover slips were incubated with anti-53BP1 antibody (Bethyl Laboratories, TX, USA) in Tris-buffered saline supplemented with 5% skim milk (TBS-DT) for 2 h at 37°C. The primary antibody was washed with PBS, and an Alexa Fluor 594–labeled anti-rabbit IgG secondary antibody (Invitrogen Ltd, California, USA) and 4',6-diamidino-2-phenylindole (DAPI; Invitrogen) were added. The cover slips were incubated for 1 h at 37°C and washed with PBS. Then, the cover slips were sealed onto glass slides with 0.03 ml PBS containing 10% glycerol (Wako). The cells were observed using a fluorescence microscope. The numbers of 53BP1 foci were counted on digitized images using Image J software.

Determination of intracellular ROS level

Intracellular ROS level was evaluated using aminophenyl fluorescein (APF) (Sekisui Medical, Tokyo, Japan). Cells were incubated with 5 μM APF for 30 min at 37°C. After 6 Gy irradiation, cells were trypsinized and resuspended in PBS. The fluorescence values of the cell suspensions were measured using a fluorescence spectrophotometer F-2700 (Hitachi, Tokyo, Japan). The excitation and emission wavelengths used were 490 nm and 515 nm, respectively.

Measurement of mitochondrial superoxide level

Mitochondrial superoxide levels were measured using Mitosox Red (Molecular Probes, Eugene, OR, USA). The cells were washed with PBS and incubated with 5 μM Mitosox Red for 30 min. After 6 Gy irradiation, cells were trypsinized and resuspended in PBS. The fluorescence values of the cell suspensions were measured using a fluorescence spectrophotometer. The excitation and emission wavelengths used were 510 nm and 580 nm, respectively.

Measurement of mitochondrial membrane potential

Mitochondrial membrane potential was measured using 5,5',6,6'-tetrachloro-1,1',3,3'-tetraethyl-benzimidazoylcarbocyanine (JC-1; Invitrogen). Briefly, cells were washed with PBS and incubated with 5 μM JC-1 for 30 min at 37°C. The green and red fluorescence values of the cell suspensions were measured using a fluorescence spectrophotometer. For green, the excitation and emission wavelengths used were 514 nm and 529 nm, respectively, and for red, the excitation and emission wavelengths used were 585 nm and 590 nm, respectively. Mitochondrial membrane potential was calculated using the rate of the red fluorescence value per green fluorescence

value. In order to show the image, cells treated with JC-1 were analyzed by using fluorescent microscopy.

Measurement of mitochondrial membrane permeability

The mitochondrial permeability transition pore (mPTP) is a non-specific channel formed by components from the inner and outer mitochondrial membranes. The opening of the mPTP dramatically alters the permeability of mitochondria. Loss of mitochondrial membrane potential is observed subsequent to continuous pore activation. We used Calcein AM, a colorless and non-fluorescent esterase substrate, and $CoCl_2$, a quencher of Calcein fluorescence, to selectively label mitochondria. Once inside cells, intracellular esterases cleave the acetoxymethyl esters to liberate the very polar fluorescent dye Calcein, which does not cross the mitochondrial or plasma membranes in appreciable amounts over relatively short periods of time. The fluorescence from cytosolic Calcein is quenched by the addition of $CoCl_2$, while the fluorescence from the mitochondrial Calcein is maintained. When mPTPs are activated, $CoCl_2$ can enter into the mitochondria, and mitochondrial fluorescence from the Calcein is quenched.

Cells were treated with 40 ng/ml IL-6 for 24 h, and harvested by trypsin. Cells were then treated with 2 μM Calcein AM (Invitrogen) and 400 μM $CoCl_2$ for 15 min at 37°C. After washing the reagent with PBS, the fluorescent values of cell suspensions (50 000 cells) were measured with a fluorescence spectrophotometer. The excitation and emission wavelengths used were 494 nm and 517 nm, respectively.

Metabolome analysis using GC/MS

To quantify intracellular metabolite (pyruvic acid and fatty acid) of cells, C6 cells were measured using a gas chromatography/mass spectrometry system (GCMS-8040; Shimazu, Kyoto, Japan). The cells in 35 mm dishes were treated (or not treated) with IL-6. Analysis was performed in accordance with the manufacturer's instructions. Briefly, cells were washed by cold saline twice and then treated with cold methanol. The methanol, containing cellular metabolites, was collected and evaporated. An aliquot of 20 μl of isopropyl malic acid (0.5 mg/ml) was added into each sample, and the metabolite was dried under reduced pressure. Pyridine solution containing 20 mg/ml methoxyamine was added into each sample, and stirred well using a voltex mixer. The sample solution was incubated with shaking at 2000 rpm for 90 min at 37°C. N-methyl-N-trimethylsilyltrifluoroacetamide (Trimethylsilylating agent) was added to the sample, and it was then incubated with shaking at 2000 rpm for 30 min at 37°C. After centrifugation at 15 000 rpm for 15 min, the supernatant was analyzed with GCMS-8040 with a fused DB-5 column (30 m × 0.25 mm inner diameter, 1 μm film thickness; Agilent Technologies, Tokyo, Japan).

Immunofluorescent staining of IL-6 receptor α (IL-6Rα)

To investigate the expression of IL-6Rα in C6 and RNB cells, they were seeded on 22 × 22 mm cover slips in 35 mm dishes. After incubating for 48 h, the cells were fixed with 4% formaldehyde in PBS. Then, the cells were permeabilized for 10 min in 0.5% Triton X-100 in PBS and washed with PBS. The cover slips were incubated with anti–IL-6Rα antibody (Bioss Inc., MA, USA) in TBS-DT for 2 h at 37°C. The primary antibody was washed with PBS, and an Alexa Fluor 488–labeled anti-rabbit IgG secondary antibody and DAPI were added. The cover slips were incubated for 1 h at 37°C and washed with PBS. Then, the cover slips were sealed onto glass slides with 0.03 ml PBS containing 10% glycerol. The cells were then observed using a fluorescence microscope.

Statistical analysis

Data were expressed as means ± standard deviations (SDs). Differences in mean values between two groups were analyzed using a two-tailed Student's t test. $P < 0.05$ was considered statistically significant.

RESULTS

IL-6 was induced in C6 cells after γ-irradiation

To investigate which cytokines were secreted after γ-irradiation in C6 and RNB cells, we performed Bio-Plex assays. The concentrations of 24 cytokines in culture medium were quantified (Supplementary Table 1). Our results showed that IL-6 was the only cytokine that increased in concentration at the every time point analyzed after 4 Gy irradiation of C6 cells (Fig. 1). On the other hand, secretion of IL-6 by RNB cells was very low. Previous reports have suggested that IL-6 participates in the acquisition of radioresistance by cancer cells; therefore, we decided to investigate IL-6 and its relationship with radioresistance in this study.

Radioresistance of C6 cells was increased by treatment with IL-6

We performed a colony-formation assay to investigate whether IL-6 participated in the acquisition of radioresistance. In the case of C6 cells, the surviving fraction of cells treated with IL-6 after 6 Gy irradiation was increased in comparison with that of non-treated control cells (Fig. 2, Supplementary Fig. 1). However, the surviving fraction of RNB cells treated with IL-6 after 6 Gy irradiation was not changed. These results suggested that IL-6 participated in the radioresistance of C6 glioma cells.

IL-6 reduces the formation of double-strand breaks after γ-irradiation

In order to measure the effects of IL-6 in the formation of DNA double-strand breaks immediately after irradiation, we examined the level of 53BP1 foci 30 min after 1 Gy irradiation (Fig. 3). As shown in Fig. 3b, treatment with IL-6 reduced the number of foci to 40% of the non-treated control level at 30 min after 1 Gy irradiation (Fig. 3). On the other hand, the number of foci at 2 and 24 h after 1 Gy irradiation was not significantly different between IL-6-treated cells and untreated cells (Fig. 3b). In the case of RNB cells, the number of foci did not differ between IL-6-treated cells and untreated cells at any time point examined after irradiation (Fig. 3b). From these results, it was thought that IL-6 inhibited a mechanism for the generation of DNA double-strand breaks.

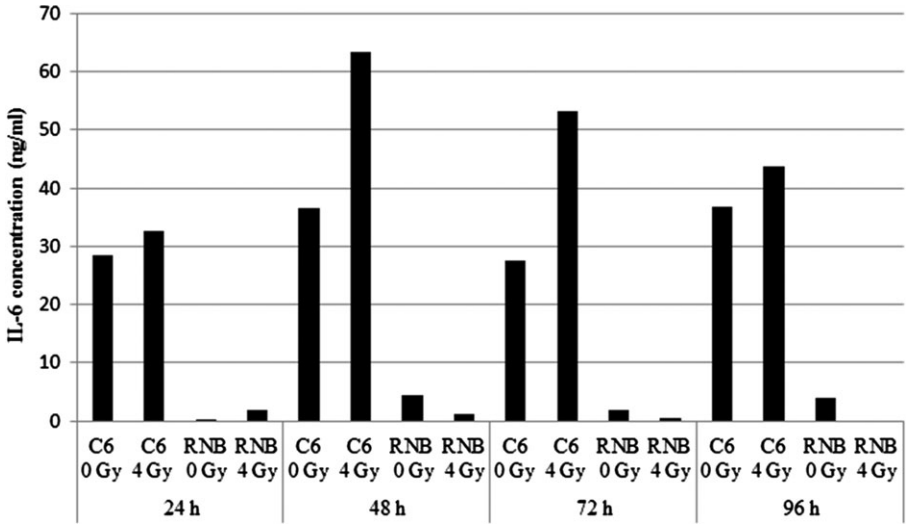

Fig. 1. Concentration of interleukin (IL)-6 in the supernatant of rat glioma cell line (C6) cells. IL-6 levels in the supernatant at 24, 48, 72 and 96 h after 4 Gy irradiation were measured using the Bio-Plex system. Data are expressed as means of duplicate samples.

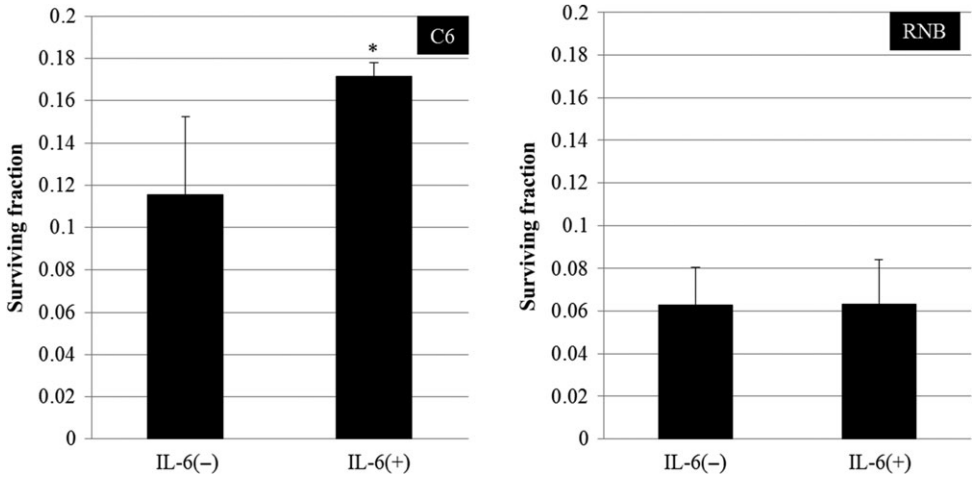

Fig. 2. Surviving fraction of cells after 6 Gy irradiation. Left and right graphs show the results for rat glioma cell line (C6) and non-tumor rat astrocyte cell line (RNB) cells, respectively. Data are expressed as the mean of three independent experiments. Significant differences were observed in C6 cells between interleukin (IL)-6 (–) and IL-6 (+) conditions (*). Error bars indicate standard deviations.

Intracellular and mitochondrial reactive oxygen species induced by irradiation were decreased by IL-6

ROS are considered to be an inducer of DNA double-strand breaks after irradiation. We examined ROS levels after 6 Gy irradiation in IL-6–treated cells. Intracellular and mitochondrial ROS were measured in immediate after IR in C6 and RNB cells (Fig. 4a). The intracellular ROS levels, detected with APF, increased in C6 and RNB cells after 6 Gy irradiation. In C6 cells, pre-treatment with IL-6 resulted in a decrease in total ROS levels by nearly 15% (Fig. 4b). The ROS level of RNB cells did not decrease after IL-6 treatment. Similarly, mitochondrial ROS levels, detected using Mitosox Red, in C6 cells were increased by 6 Gy irradiation, but the level was decreased by ~28% by IL-6 treatment (Fig. 4c). On the other hand, mitochondrial ROS levels in RNB cells were not changed by either 6 Gy irradiation or IL-6 treatment. These results suggested that IL-6 inhibited the generation of mitochondrial ROS and suppressed the induction of DNA double-strand breaks after γ-irradiation.

Mitochondrial membrane potential was inhibited by IL-6

To inspect the mechanism by which IL-6 repressed the generation of the mitochondrial ROS, we examined the membrane potential of mitochondria using the JC-1 method. The result revealed that the mitochondrial membrane potential in C6 and RNB cells was

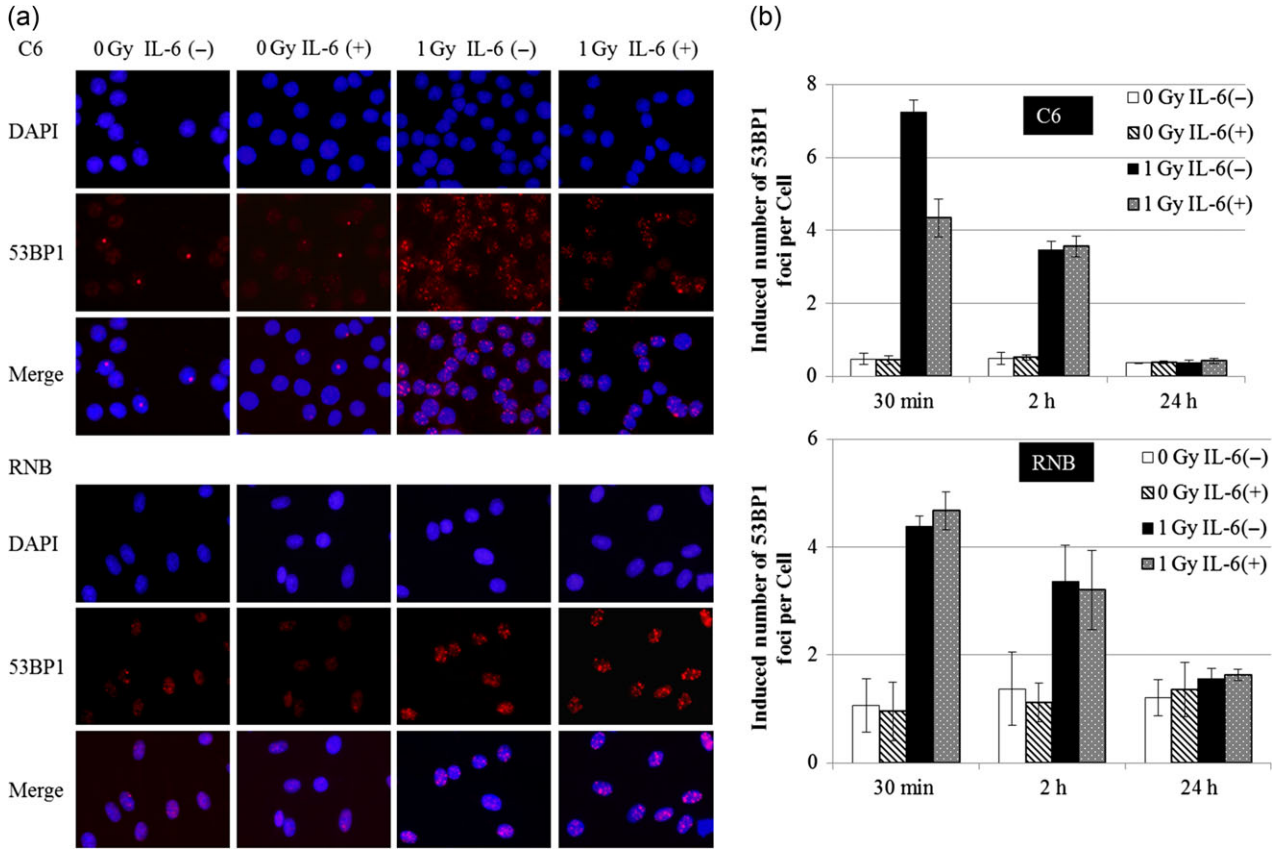

Fig. 3. 53BP1 foci of rat glioma cell line (C6) and non-tumor rat astrocyte cell line (RNB) by immunofluorescence staining. (a) Image of 53BP1 foci by immunofluorescence staining at 30 min after 1 Gy irradiation. Upper and lower panels indicate C6 and RNB cells, respectively. (b) Average number of 53BP1 foci in the nucleus at 30 min, 2 h and 24 h after 1 Gy irradiation. Upper and lower graphs show the results for C6 and RNB cells, respectively. The average of 53BP1 foci per cell was obtained from counting 200 cells in each group. Data are expressed as the mean of three independent experiments. Significant differences were observed in C6 cells between interleukin (IL)-6 (–) and IL-6 (+) conditions (*). Error bars indicate standard deviations.

decreased significantly by IL-6 treatment (Fig. 5, Supplementary Fig. 2). In addition, the mitochondrial membrane potential was decreased by 6 Gy irradiation (Fig. 5, Supplementary Fig. 2). In order to understand the mechanism of the inhibition of the membrane potential by IL-6, mitochondrial membrane permeability was investigated in C6 and RNB cells (Fig. 6). Mitochondrial membrane permeability in C6 cells was decreased significantly by IL-6 treatment, but not in RNB cells (Fig. 6). Furthermore, metabolome analysis using GC/MS was performed in C6 cells. The results showed that pyruvic acid, oleic acid and stearic acid were decreased by IL-6 treatment (Fig. 7). These results suggest that the mechanism of reductions of membrane potential differ between C6 and RNB cells.

DISCUSSION

Various phenomena such as apoptosis and DNA double-strand breaks have been reported as radiation-induced bystander effects [12–16]. It has been reported that IL-6 is one of the bystander factors [20]. In this study it was shown that IL-6 was secreted after γ-irradiation of C6 glioma cells. This study also revealed that IL-6 promoted the acquisition of radioresistance based on the suppression of DNA double-strand breaks generation. This is the first study that has demonstrated the mechanism for the relationship between IL-6 induction and acquisition of radioresistance after irradiation. In the Bio-Plex assay, we also looked at 23 cytokines other than IL-6. However, we did not examine the effects of these in the present study. In the radiation-induced bystander effect, many secreted factors are involved in complex interactions and induce phenomena such as apoptosis, DNA double-strand breaks, and the acquisition of radioresistance. It will be necessary to investigate the relationship between IL-6 and the other secreted factors to understand the radiation-induced bystander effect.

Intracellular ROS (hydroxy radicals, peroxynitrite) in cells and mitochondrial ROS (superoxide) were decreased by IL-6 treatment, and this was thought to be the main cause of the suppression of the DNA double-strand breaks after γ-irradiation. Wu *et al.* reported that ROS are derived from cytoplasm irradiation, whereas point mutations are induced in nuclear DNA [26]. This suggests that

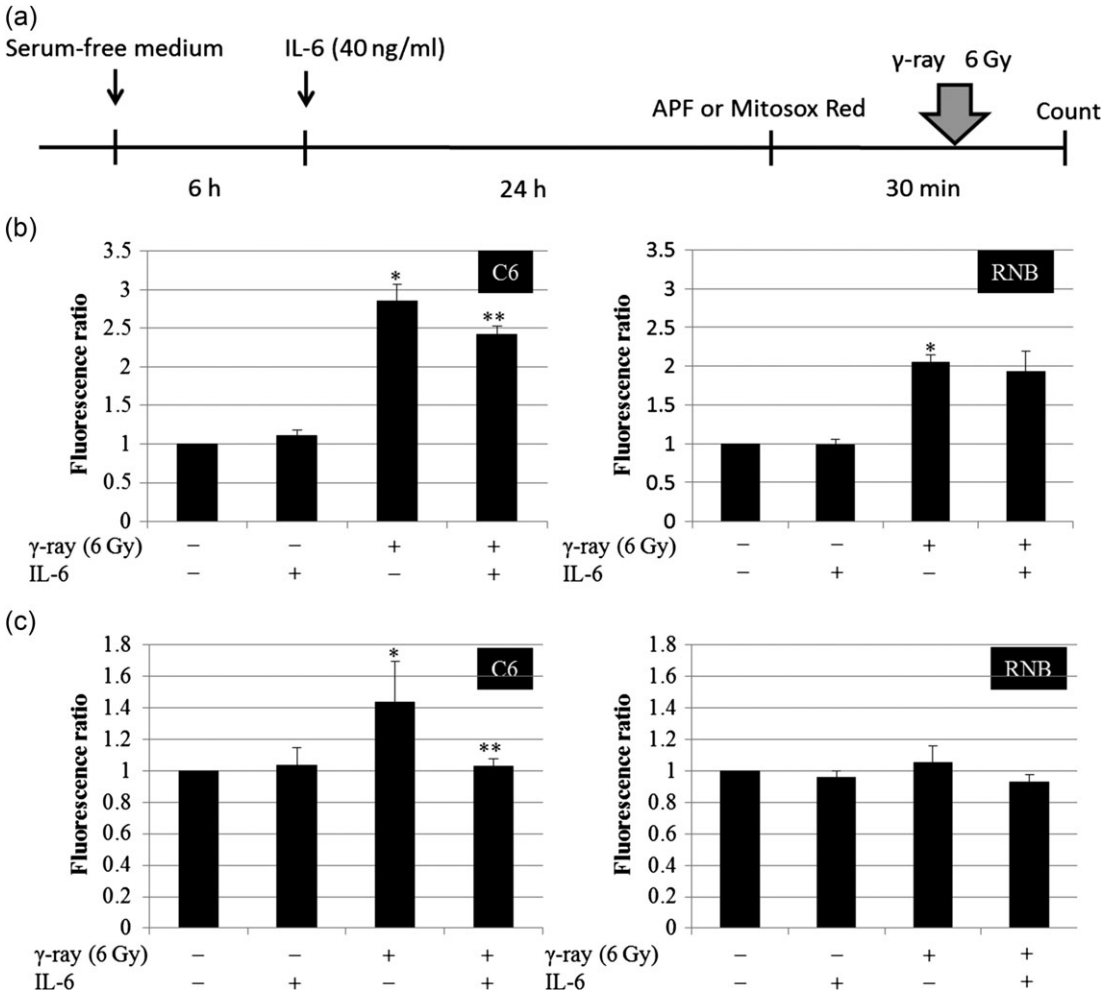

Fig. 4. Intracellular reactive oxygen species (ROS) level and mitochondrial ROS level. (a) Protocol of ROS detection is indicated. (b) Intracellular ROS levels of rat glioma cell line (C6) and non-tumor rat astrocyte cell line (RNB) cells were measured using a fluorescence spectrophotometer. Left and right graphs show the results for C6 and RNB cells, respectively. Intensity of 3′-(p-aminophenyl) fluorescein (APF) fluorescence was expressed as a relative value against that of cells without irradiation and interleukin (IL)-6 treatment. The number of cells analyzed was 5×10^5 cells. (c) Mitochondrial ROS levels in C6 and RNB cells were measured using a fluorescence spectrophotometer. The intensity of Mitosox Red fluorescence is expressed as a relative value compared with that of cells without irradiation and IL-6 treatment. The number of cells analyzed was 5×10^5 cells. Data are expressed as the mean of three independent experiments. Significant differences were observed between γ-ray (−) and γ-ray (+) conditions (*) in both C6 and RNB cells. In addition, a significant difference was observed between IL-6(−) and IL-6 (+) conditions in 6 Gy–irradiated C6 cells. Error bars indicate standard deviations.

cytoplasmic or mitochondrial ROS can induce damage in genomic DNA. It is known that superoxide converts into highly damaging ROS such as hydroxy radicals and peroxynitrite, and it has been suggested that superoxide generated in the mitochondria change into active ROS in the cytoplasm, and that this results in the genotoxic response. Therefore, it is suggested that IL-6 decreases intracellular ROS (hydroxy radicals, peroxynitrite) by inhibiting mitochondrial ROS (superoxide) and results in a reduction in the number of DNA double-strand breaks.

We examined the mitochondrial membrane potential to investigate the mechanism by which mitochondrial ROS was repressed by IL-6. Zhang *et al.* reported that complex II and complex IV of the electron transport chain are inhibited and that the production of superoxide was increased by cytoplasm irradiation [29]. Therefore, the production of superoxide in mitochondria after irradiation is thought to be related to reduction in membrane potential in mitochondria. As shown in Fig. 5, our results clarified that IL-6 and radiation exposure reduced mitochondrial membrane potential; however, they resulted in the suppression of the generation of superoxide after irradiation in C6. Therefore, the reduction of mitochondrial membrane potential may not necessarily depend on inhibition of the electron transport chain in C6 cells. We hypothesized

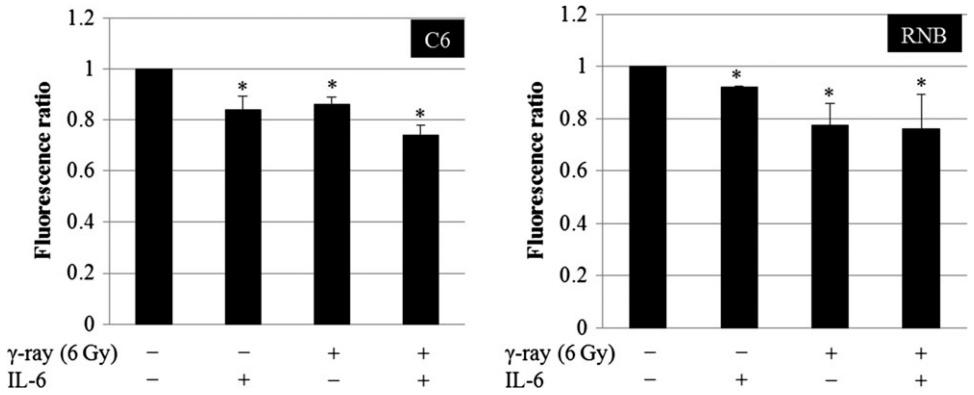

Fig. 5. Mitochondrial membrane potential of rat glioma cell line (C6) and non-tumor rat astrocyte cell line RNB cells. Left and right graphs show the results of C6 and RNB cells, respectively. Intensity of red fluorescence per green fluorescence of JC-1 is expressed as a relative value against that of cells without irradiation and interleukin (IL)-6 treatment. The number of cells analyzed was 5×10^5 cells. Data are expressed as the mean of three independent experiments. Significant differences were observed compared with control. Error bars indicate standard deviations.

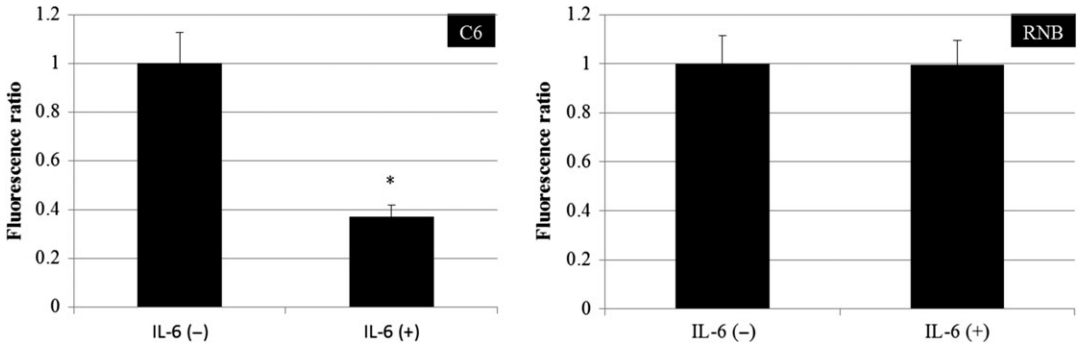

Fig. 6. Mitochondiral membrane permeability of rat glioma cell line (C6) and non-tumor rat astrocyte cell line (RNB) cells. Left and right graphs show the results of C6 and RNB cells, respectively. The number of cells analyzed was 5×10^5 cells. Data are expressed as the mean of three independent experiments. Significant differences were observed compared with control (*). Error bars indicate standard deviations.

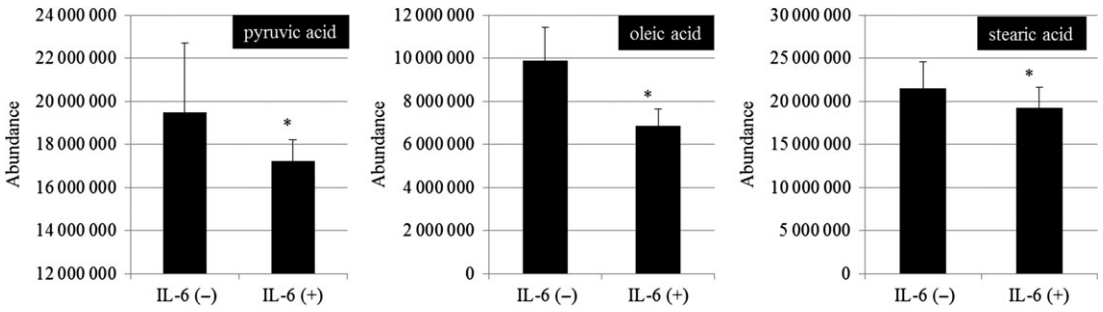

Fig. 7. Result of metabolome analysis using gas chromatography/mass spectrometry. Detected peak values were indicated the graph. Left, middle and right graphs show the results of pyruvic acid, oleic acid and stearic acid, respectively. Data are expressed as the mean of three independent experiments. Significant differences were observed compared with control (*). Error bars indicate standard deviations.

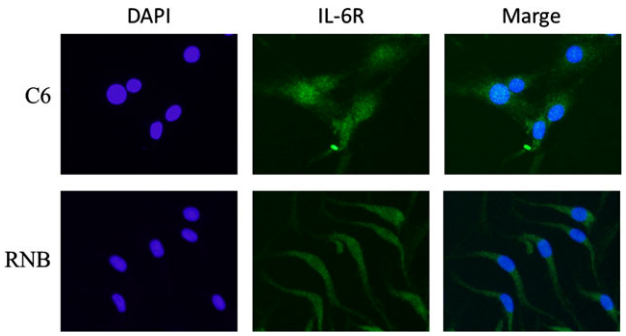

Fig. 8. Fluorescence images of interleukin (IL)-6R (green) and 4',6-diamidino-2-phenylindole (DAPI) indicating nuclei (blue). Upper and lower panels indicate rat glioma cell line (C6) and non-tumor rat astrocyte cell line (RNB) cells, respectively.

that IL-6 treatment or γ-irradiation may change the balance of metabolism for energy production in mitochondria. To clarify this, intracellular metabolomic analysis using GC/MS was carried out in C6 cells; it was found that pyruvic acid, stearic acid, and oleic acid were decreased in comparison with a control by adding IL-6 (Fig. 7). This result was supported by a previous report that IL-6 inhibits the beta-oxidation of fatty acid [30]. Therefore, it is suggested that IL-6 inhibited glycolysis, resulting in a reduced level of pyruvic acid and causing reduction in mitochondrial membrane potential. It is thought that the supply of the reduced form of NADH, which is used in the electron transport chain, was decreased by IL-6 because of a reduction in tricarboxylic acid cycle activity, resulting in reduced ROS production in mitochondria after γ-irradiation. In the case of RNB cells, the mitochondrial membrane potential was decreased by IL-6 treatment or γ-radiation, but superoxide in mitochondria was not changed by these treatments (Figs 4 and 5). To know the reason why reduced membrane potential did not lead to change in superoxide levels in RNB cells, we examined the change in mitochondrial membrane permeability by IL-6 in both C6 and RNB cells. The results showed that a significant acceleration of permeability was observed after treatment with IL-6 in C6 cells, but not in RNB cells (Fig. 6). Therefore, the mechanism of reduction of membrane potential in RNB cells would be different from that in C6 cells. Also, we investigated IL-6Rα expression, which is a key factor in signal transduction of IL-6 (Fig. 8), and the results revealed no differences in activity of the signal for IL-6 in these cell lines. Therefore, we suggest that non-tumor RNB cells were less susceptible to the regulation of membrane permeability in mitochondria by IL-6 compared with tumor C6 cells.

In summary, we demonstrated that IL-6 repressed mitochondrial ROS levels, resulting in the suppression of intracellular ROS levels, and this enhanced radioresistance by reducing DNA double-strand breaks. It is thought that mitochondrial ROS levels were repressed by IL-6, inhibiting the energy production pathway in mitochondria. Further studies are necessary to confirm the mechanism of the acquisition of radioresistance associated with IL-6.

SUPPLEMENTARY DATA

Supplementary data is available at *Journal of Radiation Research* online.

CONFLICT OF INTEREST

The authors have declared that there are no conflicts of interest.

FUNDING

This work was supported by grants for Scientific Research from the Ministry of Education, Culture, Sports, Science, and Technology in Japan (26461863).

REFERENCES

1. Kopf M, Baumann H, Freer G et al. Impaired immune and acute-phase responses in interleukin-6–deficient mice. *Nature* 1994;368:339–42, 10.1038/368339a0.
2. Liu Y, Li PK, Li C et al. Inhibition of STAT3 signaling blocks the anti-apoptotic activity of IL-6 in human liver cancer cells. *J Biol Chem* 2010;285:27429–39, 10.1074/jbc.M110.142752.
3. Liu Q, Li G, Li R et al. IL-6 promotion of glioblastoma cell invasion and angiogenesis in U251 and T98G cell lines. *J Neurooncol* 2010;100:165–76, 10.1007/s11060-010-0158-0.
4. Van Meir E, Sawamura Y, Diserens AC et al. Human glioblastoma cells release interleukin 6 *in vivo* and *in vitro*. *Cancer Res* 1990;50:6683–8.
5. Chen MF, Hsieh CC, Chen WC et al. Role of interleukin-6 in the radiation response of liver tumors. *Int J Radiat Oncol Biol Phys* 2012;84:e621–30, 10.1016/j.ijrobp.2012.07.2360.
6. Wu CT, Chen MF, Chen WC et al. The role of IL-6 in the radiation response of prostate cancer. *Radiat Oncol* 2013;8:159, 10.1186/1748-717X-8-159.
7. Chang KT, Tsai CM, Chiou YC et al. IL-6 induces neuroendocrine differentiation and cell proliferation in non–small cell lung cancer cells. *Am J Physiol Lung Cell Mol Physiol* 2005;289:446–53.
8. Dubost JJ, Rolhion C, Tchirkov A et al. Interleukin-6-producing cells in a human glioblastoma cell line are not affected by ionizing radiation. *J Neurooncol* 2002;56:29–34.
9. Azzam EI, de Toledo SM, Little JB Oxidative metabolism, gap junctions and the ionizing radiation–induced bystander effect. *Oncogene* 2003;22:7050–7, 10.1038/sj.onc.1206961.
10. Mothersill C, Seymour C. Medium from irradiated human epithelial cells but not human fibroblasts reduces the clonogenic survival of unirradiated cells. *Int J Radiat Biol* 1997;71:421–7.
11. Shao C, Furusawa Y, Aoki M et al. Nitric oxide–mediated bystander effect induced by heavy-ions in human salivary gland tumour cells. *Int J Radiat Biol* 2002;78:837–44, 10.1080/09553000210149786.
12. Prise KM, Belyakov OV, Folkard M et al. Studies of bystander effects in human fibroblasts using a charged particle microbeam. *Int J Radiat Biol* 1998;74:793–8.
13. Morgan WF, Hartmann A, Limoli CL et al. Bystander effects in radiation-induced genomic instability. *Mutat Res* 2002;504:91–100.

14. Lorimore SA, Kadhim MA, Pocock DA et al. Chromosomal instability in the descendants of unirradiated surviving cells after α-particle irradiation. *Proc Natl Acad Sci USA* 1998;95:5730–33, 10.1073/pnas.95.10.5730.
15. Lyng FM, Seymour CB, Mothersill C. Production of a signal by irradiated cells which leads to a response in unirradiated cells characteristic of initiation of apoptosis. *Br J Cancer* 2000;83: 1223–30, 10.1054/bjoc.2000.1433.
16. Kashino G, Prise KM, Schettino G et al. Evidence for induction of DNA double strand breaks in the bystander response to targeted soft X-rays in CHO cells. *Mutat Res* 2004;556:209–15, 10.1016/j.mrfmmm.2004.08.009.
17. Shao C, Stewart V, Folkard M et al. Nitric oxide–mediated signaling in the bystander response of individually targeted glioma cells. *Cancer Res* 2003;63:8437–42.
18. Iyer R, Lehnert BE. Factors underlying the cell growth–related bystander responses to alpha particles. *Cancer Res* 2000;60:1290–8.
19. Emerit I, Garban F, Vassy J et al. Superoxide-mediated clastogenesis and anticlastogenic effects of exogenous superoxide dismutase. *Proc Natl Acad Sci USA* 1996;93:12799–804.
20. Pasi F, Facoetti A, Nano R. IL-8 and IL-6 bystander signalling in human glioblastoma cells exposed to gamma radiation. *Anticancer Res* 2010;30:2769–72.
21. Ivanov VN, Zhou H, Ghandhi SA et al. Radiation-induced bystander signaling pathways in human fibroblasts: a role for interleukin-33 in the signal transmission. *Cell Signal* 2010;22: 1076–1087, 10.1016/j.cellsig.2010.02.010.
22. Narayanan PK, Goodwin EH, Lehnert BE. Alpha particles initiate biological production of superoxide anions and hydrogen peroxide in human cells. *Cancer Res* 1997;57:3963–71.
23. Woo HA, Yim SH, Shin DH et al. Inactivation of peroxiredoxin I by phosphorylation allows localized H2O2 accumulation for cell signaling. *Cell* 2010;140:517–28, 10.1016/j.cell.2010.01.009.
24. Finkel T, Holbrook NJ. Oxidants, oxidative stress and the biology of ageing. *Nature* 2000;408:239–47, 10.1038/35041687.
25. Marnett L, Plastaras JP. Endogenous DNA damage and mutation. *Trends Genet* 2001;17:214–21.
26. Wu LJ, Randers-Pehrson G, Xu A et al. Targeted cytoplasmic irradiation with alpha particles induces mutations in mammalian cells. *Proc Natl Acad Sci USA* 1999;96:4959–64.
27. Bao S, Wu Q, McLendon RE et al. Glioma stem cells promote radioresistance by preferential activation of the DNA damage response. *Nature* 2006;444:756–60, 10.1038/nature05236.
28. Hambardzumyan D, Squatrito M, Holland EC. Radiation resistance and stem-like cells in brain tumors. *Cancer Cell* 2006;10: 454–6, 10.1016/j.ccr.2006.11.008.
29. Zhang B, Davidson MM, Zhou H et al. Cytoplasmic irradiation results in mitochondrial dysfunction and DRP1-dependent mitochondrial fission. *Cancer Res* 2013;73:6700–10, 10.1158/0008-5472.CAN-13-1411.
30. Nachiappan V, Curtiss D, Corkey BE et al. Cytokines inhibit fatty acid oxidation in isolated rat hepatocytes: synergy among TNF, IL-6, and IL-1. *Shock* 1994;1:123–9.